Journal of Theoretical and Applied Vibration and Acoustics 3(1) 77-96 (2017)

I S A V

Journal of Theoretical and Applied Vibration and Acoustics

journal homepage: http://tava.isav.ir

A magnetorheological fluid damper for robust vibration control of flexible rotor-bearing systems: A comparison between sliding mode and fuzzy approaches

Ali Kamali Egoli [*], **Abdolreza Ohadi**, **Milad Kazemi Mehrabadi**

Department of Mechanical Engineering, Amirkabir University of Technology, Tehran, Iran

ARTICLE INFO

Article history:
Received 11 April 2016

Received in revised form
17 April 2017

Accepted 8 June 2017

Available online 25 June 2017

Keywords:
Rotor dynamics

Squeeze Film Damper

Magnetorheological fluid

Sliding mode

Fuzzy controllers

ABSTRACT

Squeeze Film Dampers (SFD) are commonly used for passive vibration control of rotor-bearing systems. The Magnetorheological (MR) and Electrorheological (ER) fluids in SFDs give a varying damping characteristic to the bearing that can provide active control schemes for the rotor-bearing system. A common way to model an MR bearing is implementing the Bingham plastic model. Adding this model to the finite element (F.E.) model of the rotor enables analyzing the rotor bearing behavior. In this work, considering uncertainties, three types of controllers are designed for a rotor-bearing system and the efficiency of using these controllers in attenuating the vibration amplitude of the system is studied. As a result, employing these controllers reveals a remarkable improvement in reducing the vibration amplitude of the shaft midpoint near the critical velocity.

1. Introduction

Rotating machinery, such as compressors, turbines, internal combustion engines, and electrical motors are the most widely used elements in mechanical systems. Manufacturing inaccuracy in these systems can cause the existence of unbalance forces. Vibration attenuation of rotor-bearing systems is always an interesting problem in rotor dynamics [1-4]. Using SFD in some rotor-bearing systems has a beneficial effect on the performance of the system. This is because utilizing this kind of dampers decreases the rate of vibration transmitted to the retainer structure and increases the system stability.

[*] Corresponding author:
E-mail address: alikamalie@aut.ac.ir (A. Kamali E.)

http://dx.doi.org/ 10.22064/tava.2017.39053.1043

Selecting the suitable SFD for lowering the risk of failure by fatigue and wearing leads to defining the increase in vibration as a negative effect [5, 6]. The real challenge is when it is attempted to design lighter and smaller rotor-bearing systems. Using dampers with MR fluid provides the possibility of using active and semi-active control strategies. This leads to an investigation in MR dampers in order to optimize the characteristics of dampers and designing control schemes for better results.

Electrorheological fluids are known for more than one century [7]. In the past two decades, research efforts on MR and ER fluids have resulted in industrial semi-active devices. However, only some of them are focused on the vibration control problems in rotor-bearing systems [6]. The first studies on intelligent fluids were focused on ER fluids [7, 8]. Nikolajsen [7] was the first person that used ER fluid for decreasing the vibration of a one-sided clamped rotor-bearing system. He showed that these materials are able to decrease the vibration level. Morishita and Mitsui [2] studied electrorheological dampers and concluded based on experiments that these dampers can decrease the rotating machinery vibration in a wide range of rotating speeds. They showed that for each speed, an optimum damping ratio exists which can be calculated. Tichi [9] obtained a mathematical model for a rigid rotor-bearing system with an Electrorheological (ER) damper using Reynolds equations and the Bingham model. He calculated the velocity and pressure profile for the damper and vibration attenuation near the critical speed is estimated via this model. Zhu [4] introduced a magnetorheological (MR) disc damper that worked based on the shearing mode. Then, to prove the design, they investigated the magnetic fields in the MR damper via the finite element method. It is then shown both theoretically and experimentally that the dynamic characteristics of an MR disc damper can be easily controlled by an external magnetic field. Wang et al. [6] studied the behavior of a rotor mounted on MR dampers in shear mode and achieved good results in vibration attenuation. They obtained a modified Reynolds equation set with the long bearing assumption that can predict the damper forces. They also studied the capability of an on-off controller in transverse vibration reduction. Forte et al. [10, 11] developed a linear model for a rotor-bearing system mounted on a squeeze film damper and studied the vibration behavior of such system. They modeled the magnetorheological forces with equivalent stiffness and damper values. They also investigated the effect of viscosity and critical speed on the dynamical response of the system. Kim et al. [12] designed and modeled an SFD with MR fluid using parametric identification based on the magnetic bearing working on semi-active control schemes. Hemmatian and Ohadi [1] utilized an identification model of an SFD with MR fluid with long bearing assumption and designed a robust control to reduce the vibration of the clamped rotor-bearing system with MR damper. Irannejad and Ohadi [13] studied the rotor dynamic behavior of a system and made a comparison between short bearing and long bearing assumptions for MR squeeze film dampers.

Despite the high amount of research on rotor-bearing systems, there is not any study on the performance of control algorithms with short bearing assumption. In addition, fuzzy control of rotor-bearing systems with MR dampers based on fuzzy identification is not executed yet. In this work, the mathematical model of an MR bearing is developed by simplifying the Navier-Stokes equation. Therefore, the short bearing assumption is used for simplifying the equations. This model is considered as a force that is dependent on the input current. This force is added to the finite element model of the rotor bearing system. Three kinds of semi-active controllers are applied to this model. These control schemes are model-based and reducing the vibration of the

system is considered as their goal. The performance of these controllers for controlling vibrations is also studied.

2. The magnetorheological squeeze film damper analysis

To model an SFD with MR fluid, the Navier-Stokes equation is initially considered with the assumption that viscous forces are much greater than inertial and gravitational forces. As a result, the equations are simplified as follows [14]:

$$\frac{\partial P}{\partial x} = \frac{\partial}{\partial y}(\mu \frac{\partial u_x}{\partial y}) \tag{1}$$

$$\frac{\partial P}{\partial y} = 0 \tag{2}$$

$$\frac{\partial P}{\partial z} = \frac{\partial}{\partial y}(\mu \frac{\partial u_z}{\partial y}) \tag{3}$$

In Eqs. (1-3), P is the pressure distribution and is dependent on the instantaneous angle θ of the shaft with respect to the reference coordinate system. l is the length of the MR bearing and μ is the viscosity of the fluid in the bearing. x, y and z are the coordinate axes. These parameters are shown in Fig. 1. The z axis is perpendicular to the xy plane which is not shown.

Starting from Eqs. (1-3) and considering the aforementioned assumption (short bearing), the pressure distribution is computed as follows:

$$P(\theta, z) = \begin{cases} \dfrac{6\omega\epsilon \sin\theta \left(\dot{\gamma}\mu_f + \tau_0(H)\right)}{\dot{\gamma}c^2(1+\epsilon\cos\theta)^3}(z^2 - \dfrac{l^2}{4}) & \dot{\gamma} > \dfrac{\tau_0(H)}{\mu - \mu_f} \\ \dfrac{6\omega\epsilon \sin\theta \left(\mu_p\right)}{c^2(1+\epsilon\cos\theta)^3}(z^2 - \dfrac{l^2}{4}) & \dot{\gamma} \le \dfrac{\tau_0(H)}{\mu - \mu_f} \end{cases} \tag{4}$$

where ω, ϵ and c are the whirling speed of the shaft, eccentricity and clearance between the shaft and the damper respectively. On the other hand, the MR fluid in the damper is modeled as Bingham plastic [13]. The Bingham plastic model has two regions for the conditions before and after the occurrence of the shearing phenomenon. The characteristics of this model are described by $\dot{\gamma}$, μ_f and $\tau_0(H)$ before shearing and μ_p after the shearing where μ is the viscosity defined in each zone, $\tau_0(H)$ is the yielding shearing stress that is dependent on the magnetic field intensity (H) and $\dot{\gamma}$ is the shearing stress rate. The MR bearing consists of a ball bearing around the shaft which prevents any shearing in the fluid, thus only the second part of Eq. (4) is used for simulation.

If it is assumed that the pressure distribution is zero for $\theta = 0$ to $\theta = \pi$ (Gumbel condition [15]), then the radial and tangential forces can be calculated as follows [13]:

$$F_r = \left| R \int_{-\frac{l}{2}}^{+\frac{l}{2}} \int_{\pi}^{2\pi} P \cos\theta \, d\theta \, dz \right| = \frac{2\mu_p \omega R l^3}{c^2} \frac{\epsilon^2}{(1-\epsilon^2)^2} = \mu_p B_r \tag{5}$$

$$F_t = \left| R \int_{-\frac{l}{2}}^{+\frac{l}{2}} \int_{\pi}^{2\pi} P \sin\theta \, d\theta \, dz \right| = \frac{\pi \mu_p \omega R l^3}{c^2} \frac{\epsilon}{(1-\epsilon^2)^{\frac{3}{2}}} = \mu_p B_t \tag{6}$$

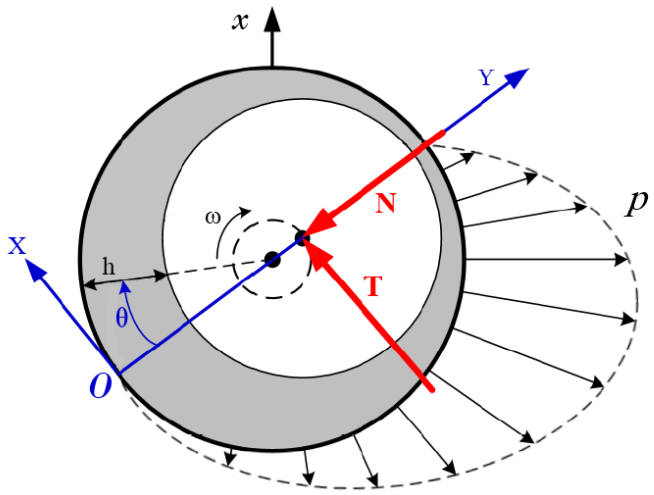

Fig. 1. Pressure distribution (P), radial and tangential forces of the bearing (N, T)

The MR damper forces can be written as a vector that has only two non-zero elements. Hence, the MR damper force is $F_{MRSFD} = \mu_p B_{MRSFD}$ where $B_{MRSFD} \in R^{n\times 1}$.

3. Rotor-bearing model

The system consists of a plane disc mounted near the midspan of an elastic shaft which is supported by two roller bearings at both sides and by a Squeeze Film Damper with magnetorheological Fluid (MRSFD) near the disc position as shown in Fig. 2-a. The system is mounted on a nonlinear elastic foundation and it is known that the MRSFD and the foundation introduce nonlinearity into the equations of motion.

The rotor is modeled using the finite element method for which 80 elements and 81 nodes (n=81) are considered. The elements are selected as Euler beam type with the length of $l_f = \frac{L}{80}$ where L is the total length of the shaft. Four degrees of freedom are considered at each node as it is seen in Fig. 2-b. The coordinate vector for each node is $q_i = [u_{xi}, u_{yi}, \theta_{yi}, \theta_{xi}]^T$ and the general coordinate vector can be considered as $x = [q_1, q_2, \dots, q_n]^T$. The lagrange's equation for each element is written where the internal damping is assumed to be negligible and boundary condition for each bearing can be considered by the Newton's law. In order to access the equation of motion for the system the equations of motion for the nodes are assembled together.

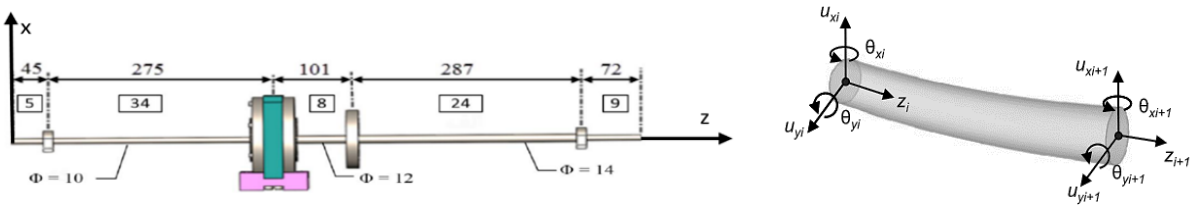

a b

Fig. 2. (a) Schemes of the rotor-bearing system with MR bearing damper. The numbers in the rectangles are the number of elements considered in the finite element model between two members. All dimensions are in mm (b) Beam element and the degrees of freedom at nodes *i* and *i+1*.

The equation of motion of this system is written as follows:

$$\boldsymbol{M\ddot{x} + C\dot{x} + Kx = F + d} \tag{7}$$

where M is the inertial matrix, C is the gyroscopic effect matrix and K is the stiffness matrix that includes both the rotor bearing and foundation. The term F includes the normal and tangential forces of the MRSFD that appear in Eq. (5) and Eq. (6). In order to use normal and tangential forces, the MRSFD force can be written in the Cartesian coordinate system. Hence, F is equal to $\left[0_{1,4*39}, F_r\cos\theta + F_t\sin\theta\,, F_r\sin\theta + F_t\cos\theta\ ,0,0,0_{1,4*41}\right]^T$. The terms 39 and 41 indicate the number of nodes before and after the MRSFD and each of the nodes has four degrees of freedom; so, the subvectors $\left[0_{1,4*39}\right]^T$ and $\left[0_{1,4*41}\right]^T$ impose zero values in F for all the nodes before and after the MRSFD. On the other hand, the subvector $[F_r\cos\theta + F_t\sin\theta\,, F_r\sin\theta + F_t\cos\theta\ ,0,0]^T$ shows that F only has nonzero values in x and y directions.

The term d is defined as the sum of the disturbances that exist in the system. Here, d denotes the combination of unbalance forces (d_1) and nonlinear forces related to the nonlinear support of the system (d_2) as $d = d_1 + d_2$. Unbalance forces can be written as $d_1 = \left[0_{1,4*47}, m_u r_u\omega^2\sin\theta\,, m_u r_u\omega^2\cos\theta, 0,0\,, 0_{1,4*33}\right]^T$ that has nonzero value on the disc node and zero in other nodes where m_u stands for mass, r_u represents the mean radius according to unbalance force and ω is the whirling speed of the shaft. The nonlinear forces that are related to the mount elasticity are defined as $d_2 = \left[0_{1,4*5}, K_{nb,x}u_{xb}^3, K_{nb,y}u_{yb}^3, 0,0, 0_{1,4*65}, K_{nb,x}u_{xb}^3, K_{nb,y}u_{yb}^3, 0,0, 0_{1,4*9}\right]^T$ which has nonzero value on the bearing nodes and zero in other nodes. $K_{nb,x}, K_{nb,y}$ are related to the mount elasticity and u_{xb} and u_{yb} are the displacements of the shaft in x and y directions at the bearing nodes. The performance of the controllers is tested in presence of these disturbances.

4. Feedback linearization control

Rotor-bearing equations of motion can be written in the following form:

$$\frac{d}{dt}\begin{Bmatrix} x \\ \dot{x} \end{Bmatrix} = \begin{bmatrix} 0 & I \\ -M^{-1}K & -M^{-1}C \end{bmatrix}\begin{Bmatrix} x \\ \dot{x} \end{Bmatrix} + \begin{Bmatrix} 0 \\ M^{-1}B_{MRSFD} \end{Bmatrix}\mu_p \tag{8}$$

$$\rho = x_{Disc}^2 + y_{Disc}^2 \tag{9}$$

where $x \in R^{4n\times 1}$ and $\dot{x} \in R^{4n\times 1}$ are the state vectors so the global state vector can be written as $X = \{x_1 \ldots . x_n . \dot{x}_1 \ldots . \dot{x}_n\}^T$. $M \in R^{4n\times 4n}$ is the inertial matrix, $K \in R^{4n\times 4n}$ is the stiffness

matrix that includes both the shaft and the foundation elasticity, $C \in R^{4n\times 4n}$ is the damping matrix and $F \in R^{4n\times 1}$ is the input vector. x_{Disc} and y_{Disc} are the horizontal and vertical displacements of the shaft at disc location and ρ is the distance of the center of the shaft from bearing axis. In this algorithm, disturbances are not considered. This means that the term d in Eq. (7) is eliminated in controller design because only their upper limit is known. However, the controller performance is evaluated in presence of disturbances. Defining $A = \begin{bmatrix} 0 & I \\ -M^{-1}K & -M^{-1}C \end{bmatrix}$, $B = \begin{Bmatrix} 0 \\ M^{-1}B_{MRSFD} \end{Bmatrix}$ and $u = \mu_p$ leads to represent Eq. (8) in the following form:

$$\dot{X} = AX + Bu \tag{10}$$

It is considered that each node has 4 degrees of freedom $x_p = \left\{x_p . y_p . \phi_{x_p} . \phi_{y_p}\right\}^T$ where ϕ_x and ϕ_y represent the rotations about x and y axes. The system is modeled with n nodes. The indices of the state vector can thus be modified based on the degrees of freedom at each node and the node number. Therefore, the output of this transformation is presented in Eq. (11).

$$\rho = x_{Disc}^2 + y_{Disc}^2 = x_{4D-3}^2 + x_{4D-2}^2 \tag{11}$$

where D is the node number related to disc location. In designing the controller, in order to obtain the relationship between ρ and u, the first and second derivatives of ρ are computed and are substituted into system equations.

$$\dot{\rho} = (x_{4D-3}\,\dot{x}_{4D-3} + x_{4D-2}\,\dot{x}_{4D-2}) = \left(x_{4D-3}\,x_{4(n+D)-3} + x_{4D-2}\,x_{4(n+D)-2}\right) \tag{12}$$

$$\ddot{\rho} = \left(\, x_{4(n+D)-3}^2 + x_{4D-3}\,\dot{x}_{4(n+D)-3} + x_{4(n+D)-2}^2 + x_{4D-2}\,\dot{x}_{4(n+D)-2}\right) \tag{13}$$

The parameters $\dot{x}_{4(n+D)-3}$ and $\dot{x}_{4(n+D)-2}$ represent the disc's accelerations in x and y directions. In other words, based on the notation given in section 3, $\dot{x}_{4(n+D)-3}$ and $\dot{x}_{4(n+D)-2}$ can be written as $\dot{x}_{4(n+D)-3} = \ddot{u}_{xD}$ and $\dot{x}_{4(n+D)-2} = \ddot{u}_{yD}$ where u_{xD} and u_{yD} are displacements of the disc. Substituting $\dot{x}_{4(n+D)-3}$ and $\dot{x}_{4(n+D)-2}$ from the equations of motion, the above equation is transformed into the following form:

$$\begin{aligned}\ddot{\rho} = \big(\, & x_{4(n+D)-3}^2 + x_{4D-3}\,(a_{4(D+n)-3}X + b_{4(D+n)-3}u) + x_{4(n+D)-2}^2 \\ & + x_{4D-2}\,(a_{4(D+n)-2}X + b_{4(D+n)-2}u)\big)\end{aligned} \tag{14}$$

In Eq. (14), a_i and b_i are defined as row matrices that represent the i[th] row of the A and B matrices. It can be written as follows:

$$\ddot{\rho} = P + Qu \tag{15}$$

where P and Q are defined in the following equations:

$$P = \left(\, x_{4(n+D)-3}^2 + x_{4D-3}\left(a_{4(D+n)-3}X\right) + x_{4(n+D)-2}^2 + x_{4D-3}\left(a_{4(D+n)-2}X\right)\right) \tag{16}$$

$$Q = (x_{4D-3}b_{4(D+n)-3} + x_{4D-2}b_{4(D+n)-2}) \tag{17}$$

Eq. (15) denotes the visible relationship of output $\ddot{\rho}$ and input u. The control input is considered in the following form:

$$u = \frac{1}{Q}(v_1 - P) \tag{18}$$

where v_1 is the auxiliary controller. Defining the error as $e = r_c - \rho$, v_1 can be designed as in the following form using the proportional derivative:

$$v_1 = k_1 e + k_2 \dot{e} \tag{19}$$

where $k_1$and k_2 are positive constants.

5. Sliding mode control

The robustness of sliding mode control can allow designing a controller with consideration of uncertainties and disturbances. In this section, the disturbance terms are added to the model and steps of designing the controller are followed. The modified model is then:

$$\frac{d}{dt}\begin{Bmatrix} x \\ \dot{x} \end{Bmatrix} = \begin{bmatrix} 0 & I \\ -M^{-1}K & -M^{-1}C \end{bmatrix}\begin{Bmatrix} x \\ \dot{x} \end{Bmatrix} + \begin{Bmatrix} 0 \\ M^{-1}B_{MRSFD} \end{Bmatrix}\mu_p + \begin{Bmatrix} 0 \\ w \end{Bmatrix} \tag{20}$$

$$y = \sqrt{x_{Disc}^2 + y_{Disc}^2} \tag{21}$$

In order to obtain the relationship between y and u, $\dot{y}$ and $\ddot{y}$ are calculated in Eq. (22) and Eq. (23) with differentiating y twice. Substituting $\dot{x}_{4(n+D)-3}.\dot{x}_{4(n+D)-2}$ from the equations of motion, the following form is obtained:

$$\begin{aligned} \dot{y} &= (x_{4D-3}^2 + x_{4D-2}^2)^{-\frac{1}{2}}(x_{4D-3}\,\dot{x}_{4D-3} + x_{4D-2}\,\dot{x}_{4D-2}) \\ &= (x_{4D-3}^2 + x_{4D-2}^2)^{-\frac{1}{2}}\left(x_{4D-3}\,x_{4(n+D)-3} + x_{4D-2}\,x_{4(n+D)-2}\right) \end{aligned} \tag{22}$$

$$\begin{aligned} \ddot{y} = (x_{4D-3}^2 + x_{4D-2}^2)^{-\frac{1}{2}}\Big(& x_{4(n+D)-3}^2 + x_{4D-3}\,(a_{4(D+n)-3}X + b_{4(D+n)-3}u + w_{4D-3}) \\ & + x_{4(n+D)-2}^2 + x_{4D-3}\,(a_{4(D+n)-2}X + b_{4(D+n)-2}u + w_{4D-2})\Big) \\ & - \frac{1}{2}(x_{4D-3}^2 + x_{4D-2}^2)^{-\frac{1}{2}}\left(x_{4D-3}\,x_{4(n+D)-3} + x_{4D-2}\,x_{4(n+D)-2}\right) \end{aligned} \tag{23}$$

For shortening the equation, P , Q and d from Eqs. (24-26) are substituted into Eq. (23).

$$\begin{aligned} P = (x_{4D-3}^2 + x_{4D-2}^2)^{-\frac{1}{2}}\Big(& x_{4(n+D)-3}^2 + x_{4D-3}\left(a_{4(D+n)-3}X\right) + x_{4(n+D)-2}^2 \\ & + x_{4D-3}\left(a_{4(D+n)-2}X\right)\Big) \\ & - \frac{1}{2}(x_{4D-3}^2 + x_{4D-2}^2)^{-\frac{1}{2}}\left(x_{4D-3}\,x_{4(n+D)-3} + x_{4D-2}\,x_{4(n+D)-2}\right) \end{aligned} \tag{24}$$

$$Q = (x_{4D-3}^2 + x_{4D-2}^2)^{-\frac{1}{2}}\left(x_{4D-3}b_{4(D+n)-3} + x_{4D-2}b_{4(D+n)-2}\right) \tag{25}$$

$$d = (x_{4D-3}^2 + x_{4D-2}^2)^{-\frac{1}{2}}(x_{4D-3}w_{4D-3} + x_{4D-2}w_{4D-2}) \tag{26}$$

Therefore, Eq. (23) is transformed into:

$$\ddot{y} = P + Qu + d \tag{27}$$

It is assumed that the sliding variable s is defined as:

$$s = \boldsymbol{ke} \tag{28}$$

where $\boldsymbol{k} = [1\ k]$, $\boldsymbol{e} = [e \quad \dot{e}]^T$ and $e = r_c - y$.

Then, the relationship between u and y is obtained and the control input can be considered as follows:

$$u = \frac{1}{Q}(v_2 - P + \eta\ sgn(s)) \tag{29}$$

where η is the higher bound of disturbances ($\eta > \max|d|$). In Eq. (29), v_2 is the auxiliary controller and it is defined in Eq. (30) as:

$$v_2 = k\dot{e} \tag{30}$$

where k is a positive constant.

6. Fuzzy controller

In the last controller, the behavior of the MR damper is identified using a fuzzy identification algorithm. In this case, B_r and B_t represent the forces of the MR damper independent of viscosity. Initially, a primary fuzzy system is created based on clustering of the inputs by Fuzzy C-means algorithm. In this system, B_r and B_t are functions of ϵ and the fuzzy system has one input and two outputs. In order to identify these forces, 70% of the data is considered as learning data and the remaining data is test data. After defining the primary fuzzy system, this model is improved by using the ANFIS toolbox in MATLAB. Results for learning the data of B_r are presented in Fig. 3 and Fig. 4. In the upper plot of Fig. 3, the output of the designed Fuzzy system ($\hat{B}_r$) and real data of the simulation are shown. It is seen that the difference between model data and real data is negligible. Given the small difference, in the lower plots of Fig. 3, the error (left plot) and the error histogram (right plot) are shown to depict a clear picture of the bounds of the error and error distribution.

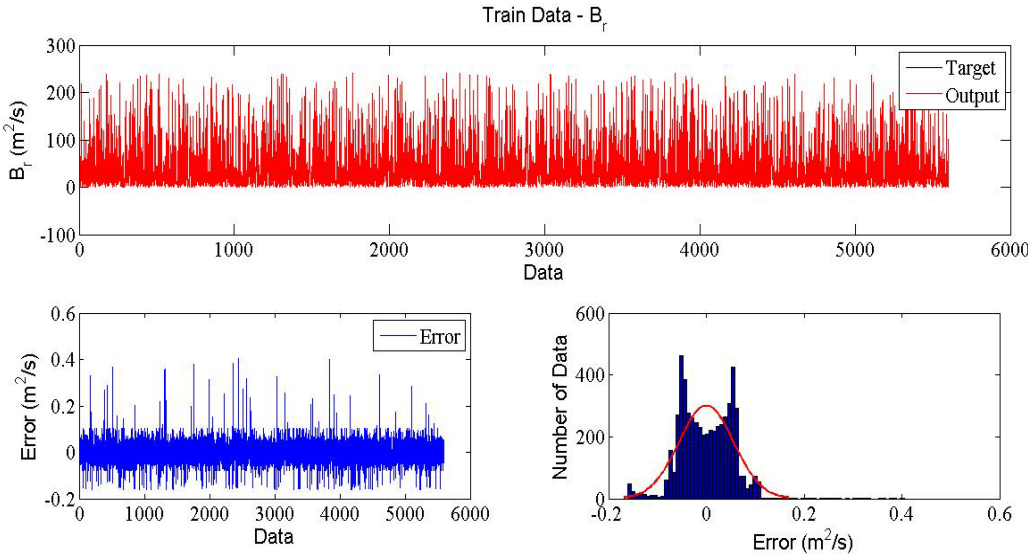

Fig. 3. Performance of the fuzzy system for training data (Br) outputs of fuzzy system vs. real values (upper plot), Error (lower left), Error's histogram (lower right)

As it can be seen in Fig. 3, the upper and lower bounds of error are 0.4 and -0.2, and the RMSE[†] is 0.056. On the other hand, the right plot is showing the resemblance of the error to the normal distribution. For a better view on the identification process, Fig. 4 shows the relationship between outputs of the fuzzy system and the real values. If a line is fit on this data, the equation of this line is Output ~= 1*Target + 6.8e−05. Therefore, it can be concluded that the fuzzy system follows the real system.

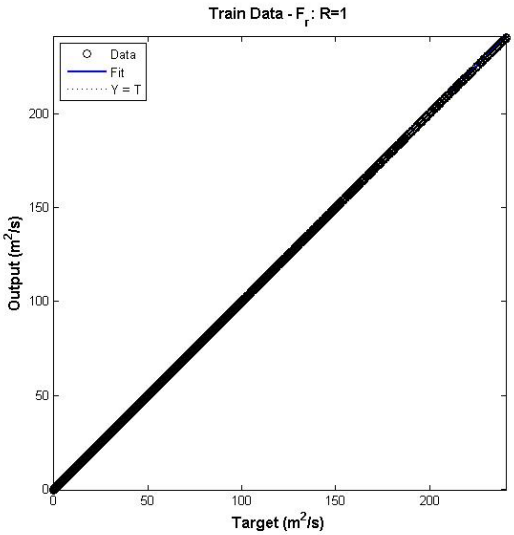

Fig. 4. Regression plot for learning data (Br)

[†] Root Mean Square Error

The results for the test data of B_r and learning and test data of B_t are presented in Table 1. As it can be seen, the identification errors of both outputs are negligible.

Table 1. Performance of Fuzzy system on the learning and test data

		RMSE	Upper Bound	Lower Bound
Training Data	B_r	0.056	0.4	-0.2
	B_t	0.027	-0.1	0.1
Test Data	B_r	0.057	0.4	-0.2
	B_t	0.027	-0.1	0.1

The behavior of the MR damper is modeled by two Takagi-Sugeno systems with membership functions of the first output (B_r) as shown in Fig. 5 and the rules of the system written as follows:

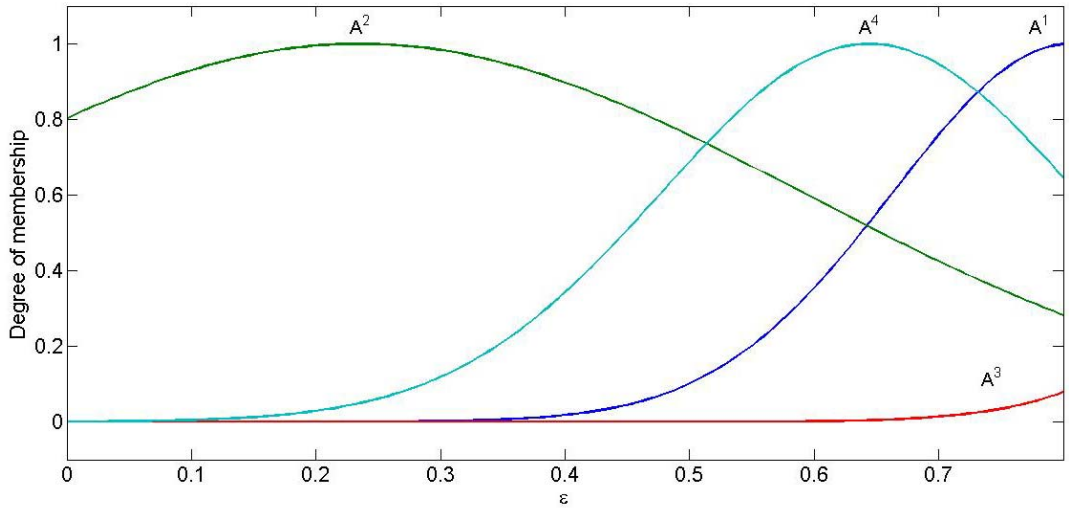

Fig. 5. Membership functions of the fuzzy system $\boldsymbol{B_r}$

$$\begin{aligned} R^{(1)}&: IF\ \epsilon\ is\ A^{(1)}\ THEN\ B_r = 362.8\epsilon\_87.82 \\ R^{(2)}&: IF\ \epsilon\ is\ A^{(2)}\ THEN\ B_r = 40.38\epsilon\_0.09645 \\ R^{(i)}&: IF\ \epsilon\ is\ A^{(3)}\ THEN\ B_r = 1829\epsilon + 1512 \\ R^{(i)}&: IF\ \epsilon\ is\ A^{(4)}\ THEN\ B_r = 52.74\epsilon + 15.3 \end{aligned} \tag{31}$$

For the second output (B_t), the membership functions are shown in Fig. 6 and the rules for each cluster are presented in Eq. (33).

$$\begin{aligned} R^{(1)}&: IF\ \epsilon\ is\ B^{(1)}\ THEN\ B_t = -0.3981\epsilon + 30.34 \\ R^{(2)}&: IF\ \epsilon\ is\ B^{(2)}\ THEN\ B_t = 229.1\epsilon - 41.89 \\ R^{(3)}&: IF\ \epsilon\ is\ B^{(3)}\ THEN\ B_t = 979.2\epsilon + 659.8 \\ R^{(4)}&: IF\ \epsilon\ is\ B^{(4)}\ THEN\ B_t = 20.96\epsilon + 43.28 \end{aligned} \tag{32}$$

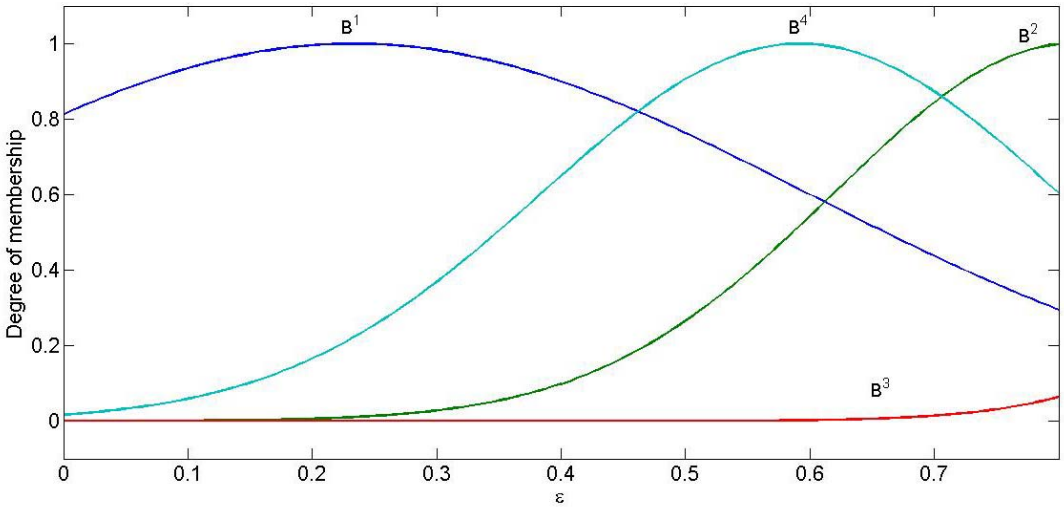

Fig. 6. Membership functions of the fuzzy system $\boldsymbol{B_r}$

In order to design the controller in Eq. (20), the disturbances are ignored and through differentiating Eq. (21) twice, the following equation can be obtained:

$$\ddot{y} = P + Qu \tag{33}$$

P and Q are defined in Eq.(24) and Eq.(25). and the controller is designed as follows

$$u = \frac{1}{Q}(v_2 - P) \tag{34}$$

In the Eq.(34) v_2 is an auxiliary controller that is defined in Eq.(30). By replacing the MR damper forces with the fuzzy system, the fuzzy controller is defined as follows:

$$R^{(i)}: IF\ \epsilon\ is\ H^{(i)}\ THEN\ u = \frac{1}{\hat{Q}}(v_2 - P) \tag{35}$$

In Eq. (35), $\hat{Q}$ is a fuzzy system based on the MR fuzzy identification process discussed.

7. Results and discussion

The parameters of the rotor-bearing system are presented in Table 2. These parameters included both the rotor-bearing system and the characteristics of the MRSFD. The output of the controller is designed for each control strategy based on the viscosity of the MR fluid. However, the electricity current is adjustable. Roszkowski et al. [16] conducted an experimental study and they concluded that there is linear relationship between the viscosity of MR fluid and the magnetic field in some regions. On the other hand, they found that there is a linear relationship between the electric current and the magnetic field ($B = \frac{\mu_0 NI}{2R}$) where μ_0 is the permeability constant, N is the number of turns of the coil and R is the mean radius of the coil.

7.1. Feedback linearization

The characteristics of the feedback linearization control are shown in Table 3. The results of the simulation are given at the spin speed of $\Omega = 1000$ rpm. There are three figures that show the trajectory of the midpoint of the disc, the distance of the midpoint of the disc from the bearing axis and the input current. All of these figures are compared with the system without a controller.

Table 2. Parameters of the rotor-bearing system [13]

Parameter	**Value**	**Parameter**	**Value**
Disc outer diameter	D=0.1 m	MRSFD length	$L = 0.016\, m$
Disc thickness	t=0.015 m	MRSFD clearance	$c = 0.001\, m$
Shaft density	ρ=7800 kg/m^3	MR fluid Newtonian viscosity	$\mu_f = 0.061\, Pa.s$
Rolling bearing stiffness, x direction y direction	 $k_x = 5e7\ N/m$ $k_y = 7e7\ N/m$	Shaft length	$L_s = 0.780\, m$
Rolling bearing damping, x direction y direction	 $C_x = 5e2\ N/m$ $C_y = 5e2\ N/m$	Shaft diameter in different positions	$D = 10; 12; 14\ mm$
Nonlinear foundation stiffness, x direction y direction	 $k_{nb,x} = 3e7\ N/m$ $k_{nb,y} = 5e7\ N/m$	Shaft Young modulus	$E = 2e11Pa$
Coil number of turns	$N = 750$	Shaft shear modulus	$G = 7.69e10\ Pa$
MRSFD average diameter	D=0.091m	Shaft Poisson's ratio	$\nu = 0.3$
		Unbalance (mass×radius)	$m_u r_u = 1e-4\ kg \cdot m$

Table 3. Parameters of the feedback linearization control

Parameter	**Value**
k_1	500
k_2	1000
r_c	$3e-4m$
Ω	1000 rpm

In Fig. 7 and Fig. 9, the efficiency of using feedback linearization control at $\Omega = 1000$ rpm is shown. As it can be seen from Fig. 9, vibration attenuation in $\Omega = 1000$ rpm is achieved by using the designed controller. The controller is trying to decrease the vibration attenuation to zero but the velocity of the shaft near the desired position is the reason that the shaft doesn't stay in that position. However, an effective attenuation is seen for the mean and maximum of the vibration amplitude. The input current, I, for the controller that is shown in Fig. (8) declared that the controller output has a high-frequency response to control the vibration of the system. On the other hand, the saturation function on the electricity current in order to keep the MR fluid behave linearly to changes in viscosity.

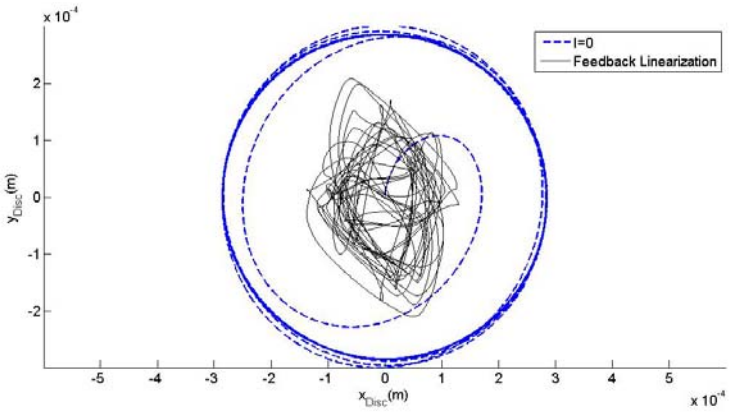

Fig. 7. Disc's midpoint trajectory in the presence of feedback linearization control and I=0

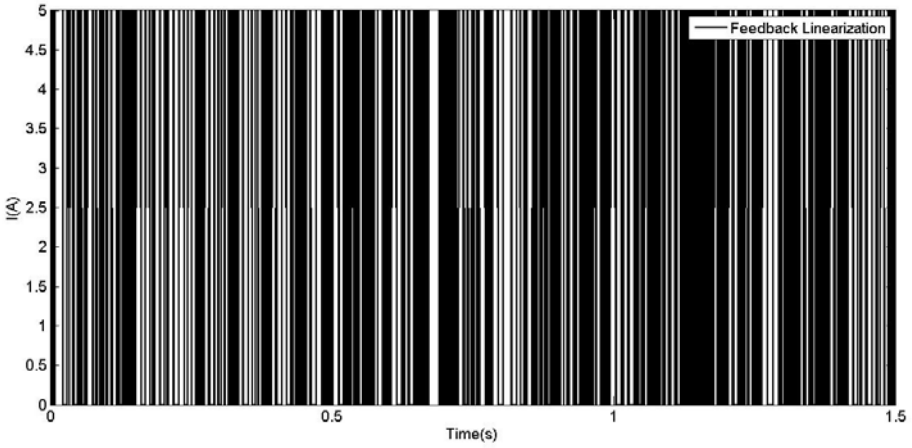

Fig. 8. Input current of the system from controller

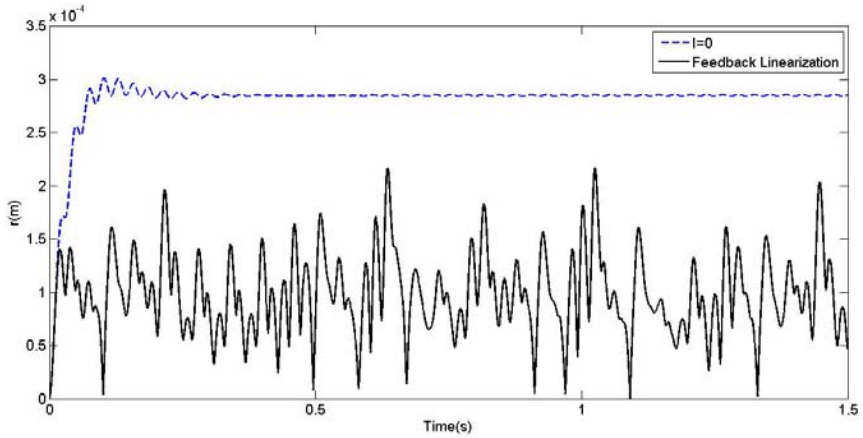

Fig. 9. Distance of the disc's center from shaft axis in terms of time for the feedback linearization control

7.2. Sliding mode control

The controller characteristics are presented in Table 4. The simulation is conducted for $\Omega = 1000$ rpm. The figures for this controller is similar to the previous section.

Table 4. Parameters of SMC feedback linearization control

Parameter	Value
k	100
r_c	0
η	2.41
Ω	1000 rpm

The vibration attenuation of sliding mode control is shown in Fig. 10 and Fig. 12. It shows that the controller is successful in decreasing the level of vibrations. In comparison with feedback linearization, this controller reaches a smoother response. The input current of MR damper is shown in Fig. 11.

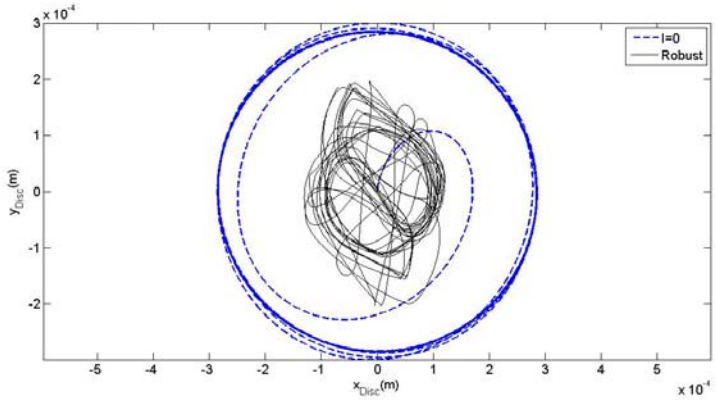

Fig. 10. Disc's midpoint trajectory in the presence of feedback linearization control and I=0

Fig. 11. Input current of the system from controller

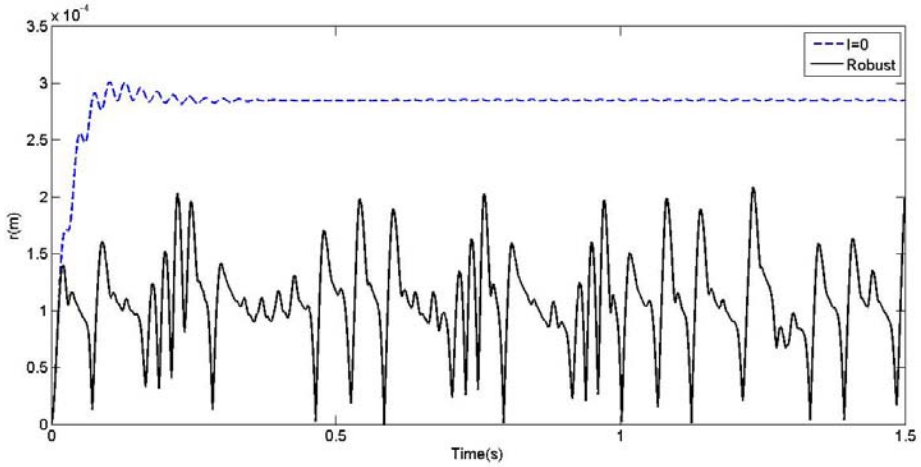

Fig. 12. Distance of the disc's center from shaft axis in terms of time in sliding mode control

7.3. Fuzzy controller

The controller characteristics are presented in Table 5. The simulation is conducted for $\Omega =$ 1000 rpm.

Table 5. Parameters of Fuzzy control

Parameter	**Value**
k	10
r_c	0
Ω	1000 rpm

The vibration attenuation of Fuzzy control is shown in Fig. 13 and Fig. 15. In this controller, smoother response is observed. The input current of the MR damper is shown in Fig. 14.

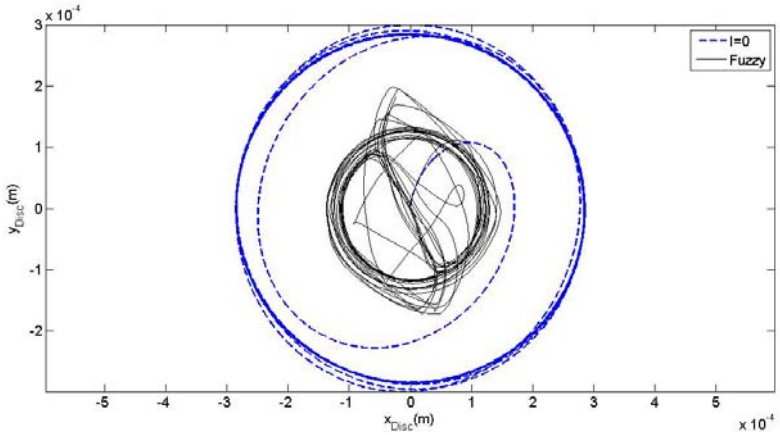

Fig. 13. Disc's midpoint trajectory in the presence of feedback linearization control and I=0

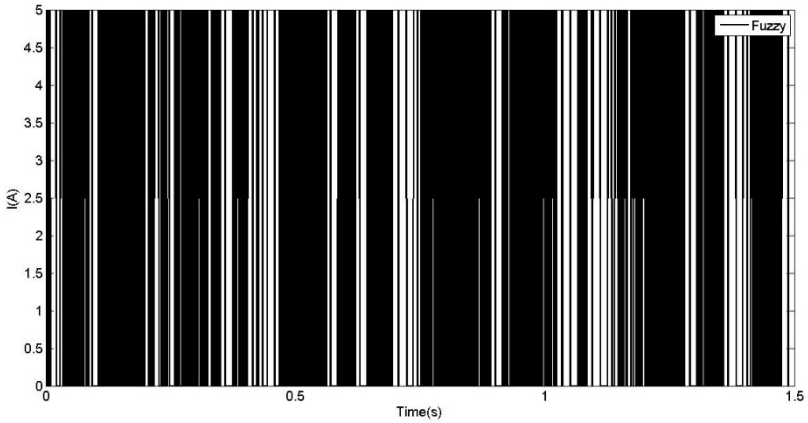

Fig. 14. Input current of the system from controller

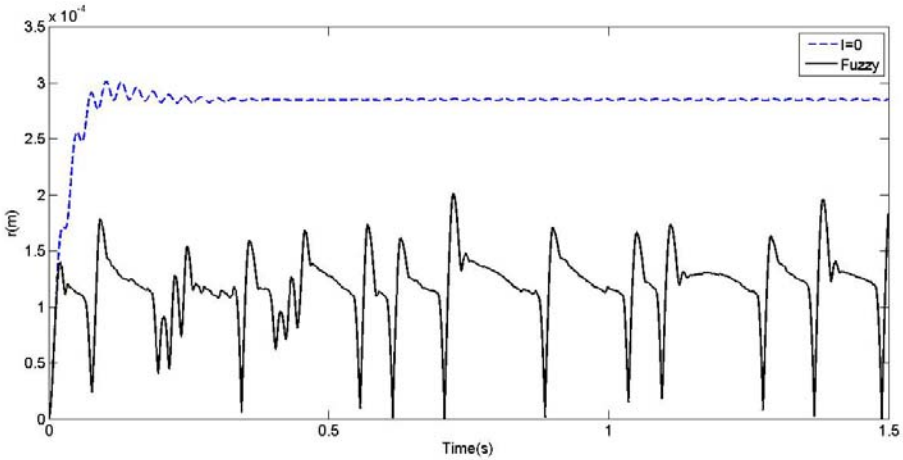

Fig. 15. Distance of the disc's center from shaft axis in terms of time for the Fuzzy control

As a comparison between the three types of controllers in Table. 6, the minimum, maximum and average values of the responses for each controller are presented.

Table 6. Performance comparison between the three types of controllers

Steady response	**Average (μm)**	**Minimum (μm)**	**Maximum(μm)**
Without controller	285	284	286
Feedback linearization	97	0.1	216
Sliding mode control	105	0.8	208
Fuzzy control	121	0.4	196

Based on Table. 6, the attenuation of vibration amplitude for all of the controllers is observed both in maximum and mean values. Moreover, the goal of designing the controllers is to test their ability in the presence of disturbances. To check this, the disturbance of the system that is related to unbalance force is changed 5%. In Fig. 16, the performance of the controllers is shown. The parameter α is the fraction of the unbalance force ($\alpha m_u r_u \omega^2$) that is defined in Table 2.

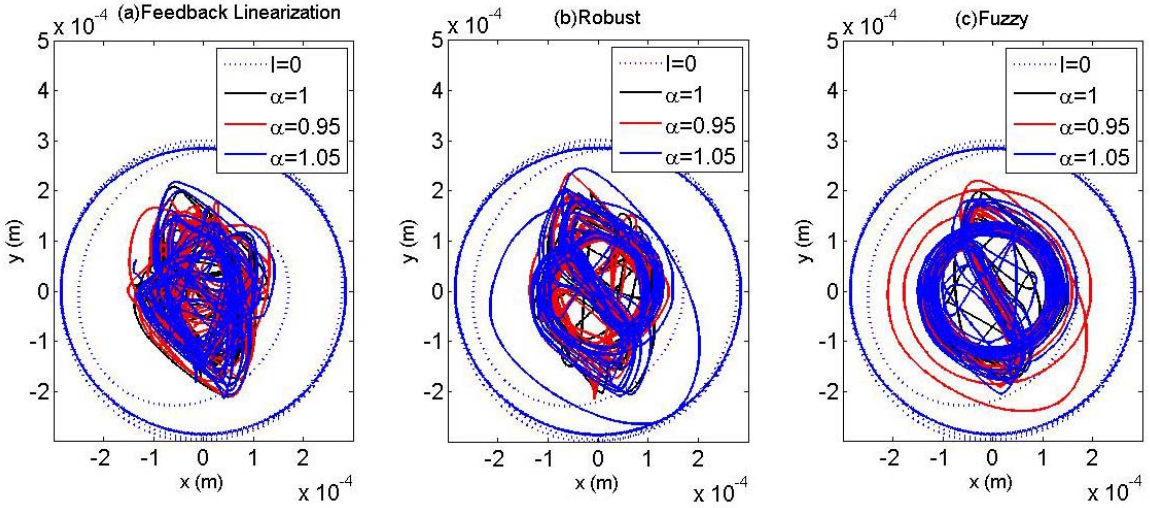

Fig. 16. Disc's midpoint trajectory in presence of different disturbance amplitudes for (a) feedback linearization control (b) Sliding mode control and (c)Fuzzy control

As it is seen, the controllers can maintain their performance after a transient response. For instance, the steady-state trajectory is less than $217\mu m$ for all investigated disturbances. The response of the system in presence of robust and fuzzy controllers is less than $214\mu m$ 6and $196\mu m$. Therefore, this can be considered as the robustness of controllers to disturbance.

On the other hand, the uncertainty in the length of the shaft is possible through the manufacturing process. Hence, the effect of the length uncertainty on the response of the rotor-bearing system in the presence of three controllers is shown in Fig. 17. The parameter α is the

fraction of the nominal length ($l_s = l \times \alpha$) and l_s is used as the shaft's length for simulation. In Fig. 17, the effect of 1% changes in the shaft length on the response of the shaft is investigated.

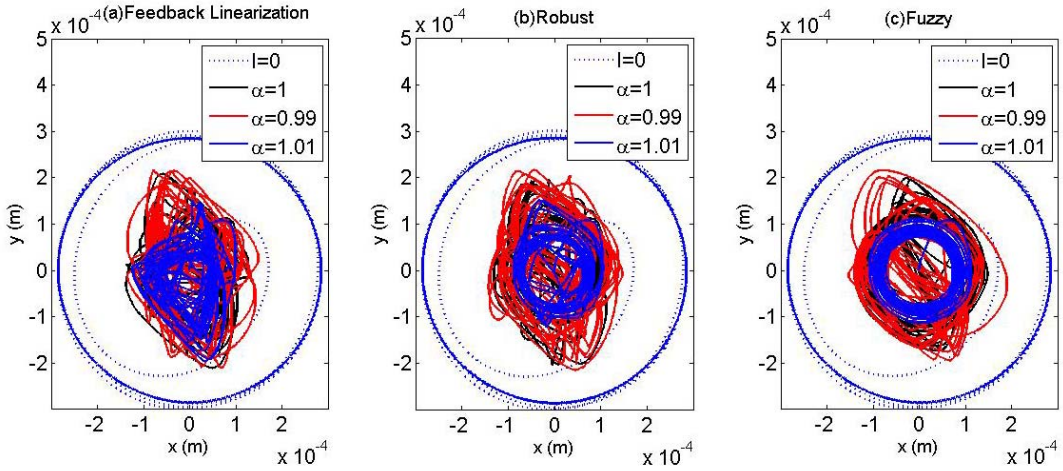

Fig. 17. Disc's midpoint trajectory in the presence of length uncertainty for (a) feedback linearization control (b) Sliding mode control and (c) Fuzzy control

Reducing the length of the shaft decreases the mass of the system. Therefore, the MR damper exerts the force on a lighter system and it causes greater amplitude in the vibration of the rotor-bearing system. However, the controllers show the capability of attenuating the amplitude of vibration. To make a comparison between controllers, one may consider that the steady response of the system for robust and fuzzy controllers is $219\mu m$ and it is less than the system with feedback linearization controller ($230\mu m$).

The characteristics of the MR fluid is not precise and the fuzzy identification of the system is based on the nominal values. So, the effect of a 5% percent change in Newtonian viscosity of the MR fluid on the performance of the system is checked in Fig. 18. The parameter α is defined as the fraction Newtonian viscosity used for simulation and the Newtonian viscosity of the MR fluid is assumed to be $\mu_f \times \alpha$.

It is clear that the controllers can keep their performance despite changes in the Newtonian viscosity. The fuzzy controller can decrease the vibration after a transient response even if the estimation of the MR forces are not based on the true viscosity. However, the robust controller is showing minimum sensitivity to this uncertainty. The steady response for feedback linearization, robust and fuzzy controllers are $217\mu m, 209\mu m$ and $196\mu m$. The response of feedback linearization does not follow a certain pattern but the system with robust and fuzzy controllers keep the shape of their response in presence of uncertainties.

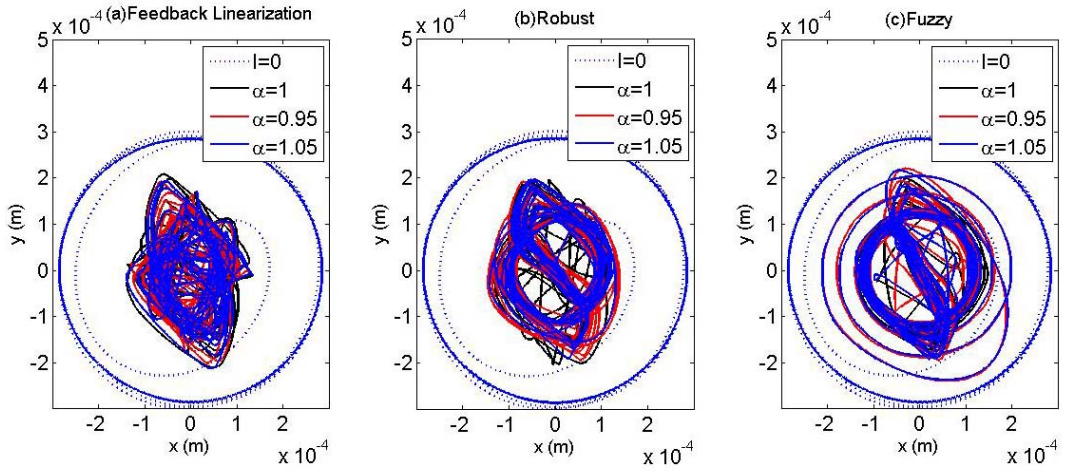

Fig. 18. Disc's midpoint trajectory in the presence of Newtonian viscosity uncertainty for (a) feedback linearization control (b) Sliding mode control and (c)Fuzzy control

8. Conclusion

In this article, the behavior of a controlled rotor-bearing system with an MRSFD is studied. In order to attenuate the vibration of the system, three controllers are designed. The model of the system is achieved by finite element modelling of the rotor-bearing system and simplifying the hydrodynamic equations of the MRSFD.

Simulation has shown that the three types of control algorithms show a beneficial performance in reducing the vibration of the shaft's midpoint. This reduction is remarkable near the critical speed of the system. On the other hand, the robustness of controllers in different disturbance amplitudes, deviation in length of the shaft and Newtonian viscosity of the MR fluid is checked and controllers are found capable of keeping their performance in attenuation.

In feedback linearization control, the amplitude reduction is up to 20%. The vibration amplitude attenuation for the sliding mode control is up to 30% and the fuzzy control has an efficiency of 33%. It is observed that considering the uncertainties in designing the controller results in a better performance for the system in vibration amplitude attenuation.

References

[1] M. Hemmatian, A. Ohadi, Sliding mode control of flexible rotor based on estimated model of magnetorheological squeeze film damper, Journal of Vibration and Acoustics, 135 (2013) 051023.
[2] S. Morishita, M. Jun'ichi, Controllable squeeze film damper (An application of electro-rheologioal fluid), Journal of Vibration and Acoustics, 114 (1992) 354-357.
[3] J. Wang, G. Meng, Study of the vibration control of a rotor system using a magnetorheological fluid damper, Journal of Vibration and Control, 11 (2005) 263-276.
[4] C. Zhu, A disk-type magneto-rheological fluid damper for rotor system vibration control, Journal of Sound and Vibration, 283 (2005) 1051-1069.
[5] A. Harnoy, Bearing design in machinery: engineering tribology and lubrication, CRC press, 2002.
[6] J. Wang, G. Meng, N. Feng, E.J. Hahn, Dynamic performance and control of squeeze mode MR fluid damper–rotor system, Smart Materials and Structures, 14 (2005) 529.

[7] J. Nikolajsen, M. Hoque, An electroviscous damper for rotor applications, Journal of Vibration and Acoustics, 112 (1990) 440-443.
[8] M. Guang, F. Tong, Q. Yang, Electro-rheological multi-layer squeeze film damper and its application to vibration control of rotor system, Journal of Vibration and Acoustics, 122 (2000) 7-11.
[9] J.A. Tichy, Behavior of a squeeze film damper with an electrorheological fluid, Tribology transactions, 36 (1993) 127-133.
[10] P. Forte, M. Paternò, E. Rustighi, A magnetorheological fluid damper for rotor applications, International Journal of Rotating Machinery, 10 (2004) 175-182.
[11] C. Carmignani, P. Forte, E. Rustighi, Design of a novel magneto-rheological squeeze-film damper, Smart Materials and Structures, 15 (2006) 164.
[12] K.J. Kim, C.W. Lee, J.H. Koo, Design and modeling of semi-active squeeze film dampers using magneto-rheological fluids, Smart Materials and Structures, 17 (2008) 035006.
[13] M. Irannejad, A. Ohadi, Vibration analysis of a rotor supported on magnetorheological squeeze film damper with short bearing approximation: A contrast between short and long bearing approximations, Journal of Vibration and Control, (2015) 1077546315601298.
[14] P.R. Childs, Rotating flow, Elsevier, 2010.
[15] Y. Ishida, T. Yamamoto, Linear and nonlinear rotordynamics: a modern treatment with applications, John Wiley & Sons, 2013.
[16] A. Roszkowski, M. Bogdan, W. Skoczynski, B. Marek, Testing viscosity of MR fluid in magnetic field, Measurement Science Review, 8 (2008) 58-60.